World Journal of Advanced Research and Reviews
eISSN: 2581-9615 CODEN (USA): WJARAI
Cross Ref DOI: 10.30574/wjarr
Journal homepage: https://wjarr.com/

(RESEARCH ARTICLE)

Check for updates

Mapping and analysis of land subsidence in Awka south L.G.A using sentinel 1 data

Njoku Richard Ebere [1], Igbokwe Esomchukwu Chinagorom [2,*], Ezeh Francis Chukwuemeka [2] and Oliha Andrew Osagie [2]

[1] *Department of Surveying and Geoinformatics, Federal University of Technology Owerri, Nigeria.*
[2] *Department of Surveying and Geoinformatics, Nnamdi Azikiwe University Awka, Nigeria.*

World Journal of Advanced Research and Reviews, 2024, 22(03), 528–536

Publication history: Received on 01 May 2024; revised on 08 June 2024; accepted on 10 June 2024

Article DOI: https://doi.org/10.30574/wjarr.2024.22.3.1749

Abstract

This study mapped and analysed land subsidence in Awka South, Anambra State, Nigeria with the view of determining the trend and rate of ground displacements within the study area. Its objectives are to model and analyze time-dependent ground displacements of Awka between 2019 and 2020; ascertain the trend, of the ground displacements between 2019 and 2020; determine the vulnerability of land subsidence in Awka South between 2019 and 2020 and to develop an inventory map to show land subsidence susceptibility areas in Awka South. The methodology involved TopSAR Split to split each sub swath with selected bursts into a separate product, application of Orbit File to acquire the satellite orbit file, back Geocoding to co-registers the four S-1 SLC split products (January and December of 2019 and that of 2020) of the same sub-swath using the orbits of the two products, enhanced spectral diversity to implement the network enhanced spectral diversity (NESD) method for TOPS coregistration, interferogram to compute (complex) interferogram, deburst to limited the results to the burst covering the study area, phase removal to estimate and subtract topographic phase from the interferogram, multilook and Goldstein Phase Filtering and Unwrap Phase to reduce speckle noise the residues in the phase unwrapping step respectively then displacement and range doppler terrain corrections to convert interferometric phase to displacement map. The results showed that subsidence in Awka South was ranging between a minimum of 2.33m to a maximum of 9.76m in 2019 and a minimum of 3.99m to a maximum of 11.22m in 2020. The results also indicated that Awka South had a trend of change of 6.95 % at the annual rate of change of 3.47m/y. The results indicated an expanding/increasing Subsidence in Awka South. The results obtained from the Land Subsidence vulnerability revealed high-risk zone occupied 33% of the entire area, spanning 5634.78 hectares, while Moderate risk zone occupied 16.18% spanning 2763.47 hectares while low risk zone occupied 50.82% spanning of 8678.22 hectares. The maps provided in this study is recommended as a spatial data addition for a decision support system on land subsidence issues.

Keywords: Ground Deformation; InSAR; Land Subsidence; Remote Sensing; Risk Assessment; Sentinel-1

1. Introduction

Land subsidence, a gradual settling or sudden sinking of the Earth's surface, poses significant challenges to infrastructure, water resources, and environmental stability. It can result from natural processes such as tectonic activities, as well as human activities including groundwater extraction, mining, and oil and gas extraction (Galloway & Burbey, 2011). In urban areas, subsidence can lead to severe damage to buildings, roads, and other infrastructure, exacerbating the costs of maintenance and repair (Chaussard et al., 2013).

Awka South Local Government Area (LGA) in Nigeria has witnessed notable instances of land subsidence, largely attributed to anthropogenic activities such as extensive groundwater extraction and construction activities (Alozie et

* Corresponding author: Igbokwe EC

al., 2020). Understanding and mapping the extent of subsidence in this region is crucial for urban planning and risk management.

Recent advances in remote sensing technologies, particularly the use of Synthetic Aperture Radar (SAR) data from satellites like Sentinel-1, have revolutionized the ability to monitor and analyze land subsidence with high precision (Ferretti et al., 2001). Sentinel-1, part of the European Space Agency's Copernicus Program, provides continuous and accurate data suitable for Interferometric Synthetic Aperture Radar (InSAR) analysis, which is effective for detecting ground deformation over large areas (Raucoules et al., 2009).

InSAR techniques allow for the detection of millimeter-scale changes in land elevation by analyzing the phase difference between multiple SAR images taken over time (Hanssen, 2001). This capability makes it an invaluable tool for monitoring subsidence in urban environments where ground deformation can have critical consequences (Hooper et al., 2012).

Previous studies have successfully utilized Sentinel-1 data to monitor subsidence in various parts of the world. For instance, Tomás et al. (2014) demonstrated the effectiveness of Sentinel-1 in mapping subsidence in urban areas of Spain, while Raspini et al. (2018) highlighted its use in detecting ground deformation in Italy. These studies underscore the potential of Sentinel-1 data in providing detailed insights into subsidence dynamics.

In Nigeria, research on land subsidence has been relatively limited, with most studies focusing on groundwater depletion and its effects (Olorunfemi et al., 2011). However, the increasing availability of high-resolution satellite data presents new opportunities for comprehensive subsidence mapping and analysis in regions like Awka South.

This study aims to leverage Sentinel-1 SAR data to map and analyze land subsidence in Awka South LGA, providing a detailed assessment of subsidence patterns and their implications. By employing advanced InSAR processing techniques, this research seeks to contribute to the growing body of knowledge on subsidence monitoring and support the development of effective mitigation strategies in the region.

The significance of this research lies in its potential to inform urban planning and infrastructure management in Awka South. With accurate subsidence data, policymakers and planners can implement measures to mitigate the impacts of subsidence, ensuring the safety and sustainability of the area's development (Galloway et al., 1999).

2. Materials and Methods

2.1. Study area

Awka South is a local government in Anambra State, it lies within latitude 6°10'N and 6°15' N of the Equator and longitude 7°02'E and7°07'E of the Greenwich Meridian. It covers a total land area of about 73 square kilometers. Awka South has a population of approximately 2.5 million which comprises Awka town and settlements such as Amawbia, Ifite-Awka, Isiagu, Mbaukwu, Nibo, Nise, Okpuno and Umuawulu.

Awka lies in the rain forest zone of Nigeria with a mean annual rainfall of 1828 mm and with an average temperature of 27° C. The relative humidity ranges between 85 and 100% during the rainy season and less than 70% during the dry season. The pattern of rainfall is bimodal, the first peak occurring in June-July, and the second in September with a little dry spell in August. In the geology, Awka in Anambra State lies within the Anambra Basin whose sedimentary rocks are made up of Nkporo Shale, the Mamu Formation, the Ajali sandstone and the Nsukka Formation as the main deposits. On the surface, the dominant sedimentary rocks are the Imo Shale, which is a sequence of grey shales with occasional clay iron stones and sandstone beds. The Imo Shale underlies the eastern part of the State, particularly in Ayamelum, Awka North, and Oruma North Local Government Areas. Below the Imo Shale is the Ameke Formation, which includes Nanka Sands.

2.2. Methods

2.2.1. Data Requirements and Acquisition

The research utilized Sentinel-1 time series data, specifically obtained from the Open Access Hub (copernicus.eu). This data is critical for understanding changes over time and provides a robust foundation for InSAR processing and analysis.

2.2.2. Processing Techniques

- TOPSAR Split

The first step in the InSAR processing chain involved the use of the TOPSAR Split technique, which divides each sub-swath with selected bursts into separate products. This division is crucial for managing the large datasets typically associated with Sentinel-1 imagery and ensures that subsequent processing steps can be performed more efficiently.

- Apply Orbit File

Following the split, the next step was to apply the precise orbit file to update the satellite's position and velocity information. The initial orbit state vectors in the SAR product metadata are often imprecise, and refining them with accurate orbit files—available several days to weeks post-generation—ensures higher accuracy in data analysis. This step is vital because accurate satellite positioning enhances the reliability of the entire processing chain.

- Back Geocoding

Back geocoding was performed to co-register two S-1 SLC split products, such as those from January and December of 2019 and 2020, of the same sub-swath. This process uses the orbits and a Digital Elevation Model (DEM) to align the slave images with the master frame. Initially, deramping and demodulation are applied to the slave image, followed by truncated-sinc interpolation, and finally reramping and remodulation to complete the co-registration. This step is crucial for ensuring spatial consistency across different time points, which is fundamental for accurate change detection and analysis.

- Enhanced Spectral Diversity

To improve coregistration accuracy, the Network Enhanced Spectral Diversity (NESD) method, was implemented. This method creates a network of images and solves an optimization problem to estimate rigid azimuth and range offsets with respect to a master image. By considering the offsets of multiple slave-slave pairs, this technique ensures high precision in aligning images, which is essential for detecting subtle changes in the landscape.

- Interferogram Generation

Interferograms were generated to measure phase differences, with the option to subtract the flat-earth phase. The flat-earth phase, caused by the curvature of the reference surface, was estimated and subtracted using a 2D polynomial. Typically, a 5th-degree polynomial was sufficient to model this phase over a full SAR scene, although the degree could vary depending on image size and coverage area. This step is critical for isolating the phase changes related to surface deformation from those due to the Earth's curvature.

- Deburst

For the SAR SLC products, each swath and polarization combination results in a product that consists of a series of bursts. For IW products, which have three swaths, and EW products, which have five, each sub-swath image was processed as a separate SLC image. The bursts, which are individually focused, were re-sampled to a common grid to ensure consistent pixel spacing. This debursting process ensures that the final images are seamless and accurately represent the observed area.

- Topographic Phase Removal

After generating the interferogram, the topographic phase was estimated and subtracted using a DEM. This process, known as topographic phase removal, adjusts the interferogram to account for variations in elevation, thereby isolating the phase related to surface movement. This step is essential for accurate deformation analysis as it removes the influence of terrain elevation.

- Multilook Processing

Multilook processing was employed to reduce speckle noise inherent in SAR images. By averaging a single look image with a sliding window, this technique enhances image interpretability and produces application products with nominal pixel sizes. This step is particularly important for improving the quality of the final images, making them more suitable for detailed analysis.

- Goldstein Phase Filtering and Unwrap Phase

To reduce residues in the phase unwrapping step and enhance accuracy, the Goldstein and Werner (1998) nonlinear adaptive algorithm was applied. Phase filtering is a critical preprocessing step that ensures the phase unwrapping process is more accurate, which is vital for precise deformation measurement.

- Displacement and Range Doppler Terrain Correction

Finally, the processing involved correcting for terrain-induced distortions and converting interferometric phase to displacement maps. This step accounted for changes in scatterer positions between SAR observations, such as those caused by subsidence, landslides, or earthquakes. By removing topographic phase and flattening the interferogram, the resultant phase map reflects only relative terrain displacement. Terrain correction ensured that the geometric representation of the image closely matched real-world conditions, which is essential for accurate spatial analysis and interpretation.

3. Results

3.1. Extent of Land Subsidence in Awka South Between 2019 and 2020

In mapping the extent of land subsidence in Awka South, four Sentinel 1A SAR images were used. These images went through a series of InSAR processing to determine the TopoPhase and Coherence product, these products were terrain corrected using range doppler terrain corrections, then displacement was calculated from the products.

From the results, the extent showed that the subsidence was ranging between a minimum of 2.33m to a maximum of 9.76m in 2019 and a minimum of 3.99m to a maximum of 11.22m in 2020. This is illustrated in figure 1, Figure 2 and figure 3.

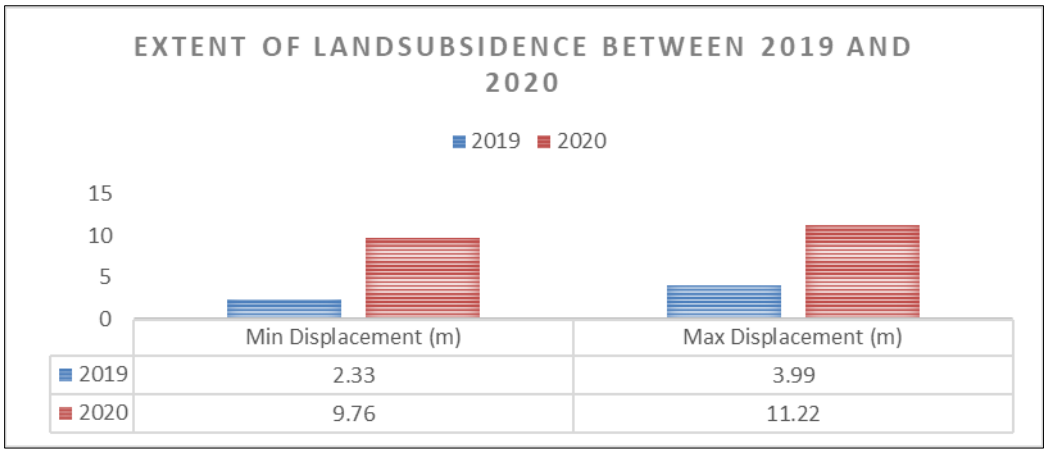

Figure 1 Land Subsidence between 2019 and 2020

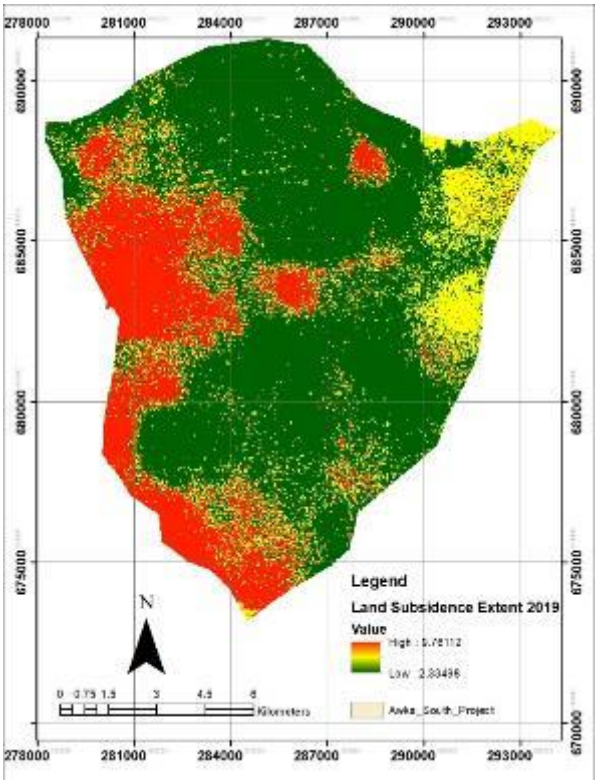

Figure 2 Land Subsidence Extent in 2019

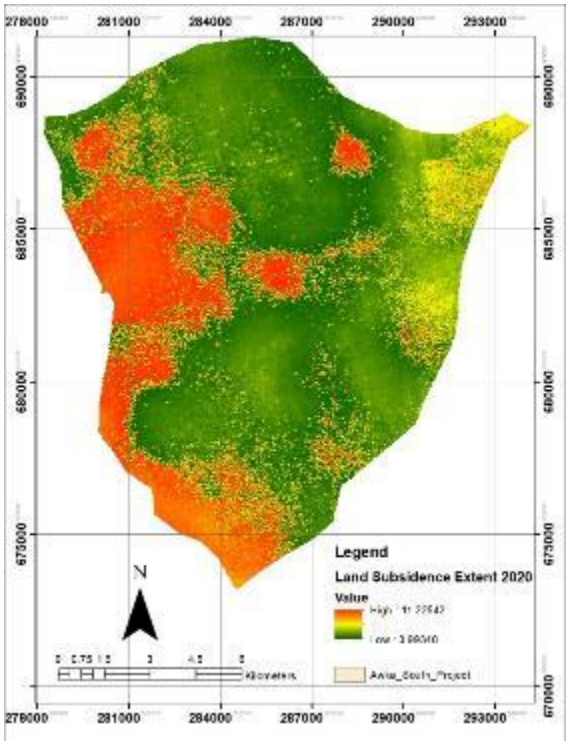

Figure 3 Land Subsidence Extent in 2020

3.2. Trend and Annual Rate of Land Subsidence between 2019 and 2020

Long *et al*., 2007's method of calculating and comparing the displacements of each year was adopted for data analysis. The comparison of the displacement statistics assists in identifying the general ground movement between 2019 and 2020. In achieving this, a table was prepared showing the ground movements and percentage change for each year

measured against each other. To determine the rate of movement, the year periods 2019 and 2020 compared against each other.

Percentage change to determine the trend of change can be calculated by dividing the observed change by the sum of the ground movements in that period multiplied by 100

$$(\text{Trend})\ \%\ \text{change} = \frac{\text{Observed change}}{\text{Total displacement}} \times 100 \qquad \ldots (1)$$

Where Observed change = (Displacement of after year – Displacement of before year)

Total Displacement = Total Displacement of both years

The annual percentage rate = Trend divided by N (number of years).

A trend percentage with a value greater than zero means that subsidence has increased over the period of years while a value less than zero shows a decrease in subsidence over a period of time.

The analysis of trend percentage and annual growth rate of the land subsidence between 2019 and 2020 as computed is shown in table 1, 2 and illustrated in figure 4.

Table 1 Difference and Total Displacement of the Awka South between 2019 and 2020

Class Type	**Difference (m)**	**Total Displacement (m)**
	2019 - 2020	2019 - 2020
Awka South	-1.46	20.98

In this study, between 2019 and 2020, the difference in ground movements (table 4.2) was 1.46m, while the total displacement was 20.98m between 2019 and 2020.

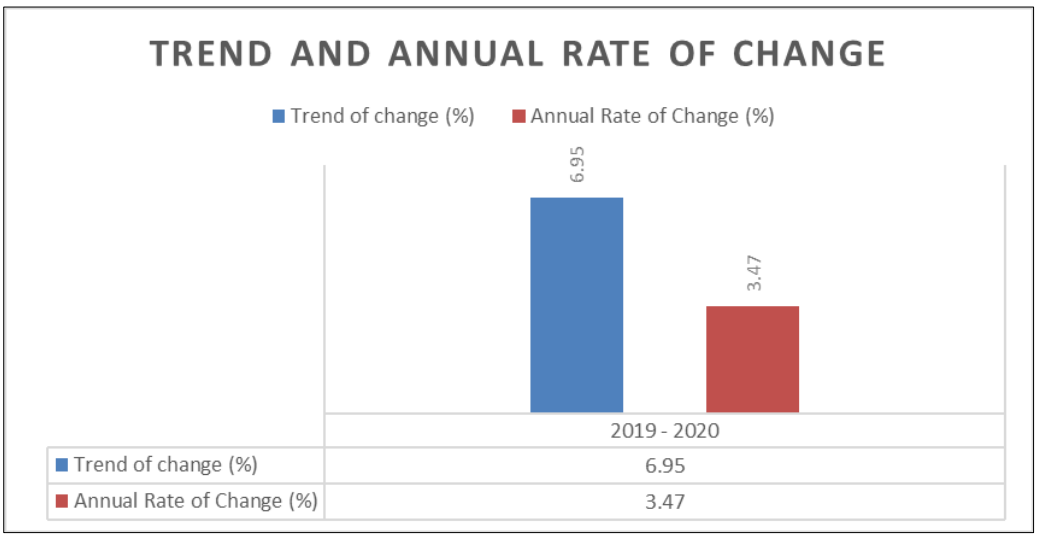

Figure 4 Trend and Annual rate of change of Awka South between 2019 and 2020

From table 1, 2 and figure 4, it can be seen that between 2019 and 2020, the Awka South had a trend of change of 6.95 % at the annual rate of change of 3.47m/y. The results indicated an expanding/increasing Subsidence in Awka South, as seen also in figure 4.3

Table 2 Difference length of change and Annual rate of change of subsidence

Class Type	Trend of Change (%)	Annual Rate of Change (%)
	2019 - 2020	2019 - 2020
Awka South	6.95	3.47

3.3. Land Subsidence Vulnerability in Awka South LGA.

Land subsidence vulnerability values obtained in the net displacement movement were reclassified into three vulnerability levels; namely high risk, moderate risk and low using natural breaks (jenks) and the percentages and areas covered were extracted. The results obtained from the Land Subsidence vulnerability revealed high-risk zone occupied 33% of the entire area, spanning 5634.78 hectares, while Moderate risk zone occupied 16.18% spanning 2763.47 hectares while low risk zone occupied 50.82% spanning of 8678.22 hectares, see figures 5 and 6.

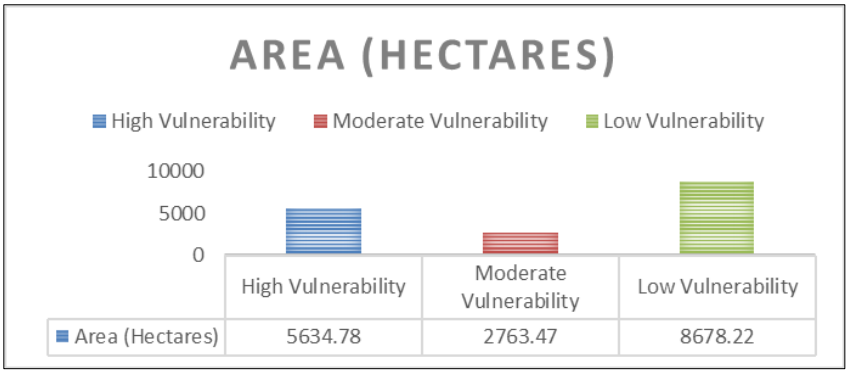

Figure 5 Land Subsidence Vulnerability Distribution

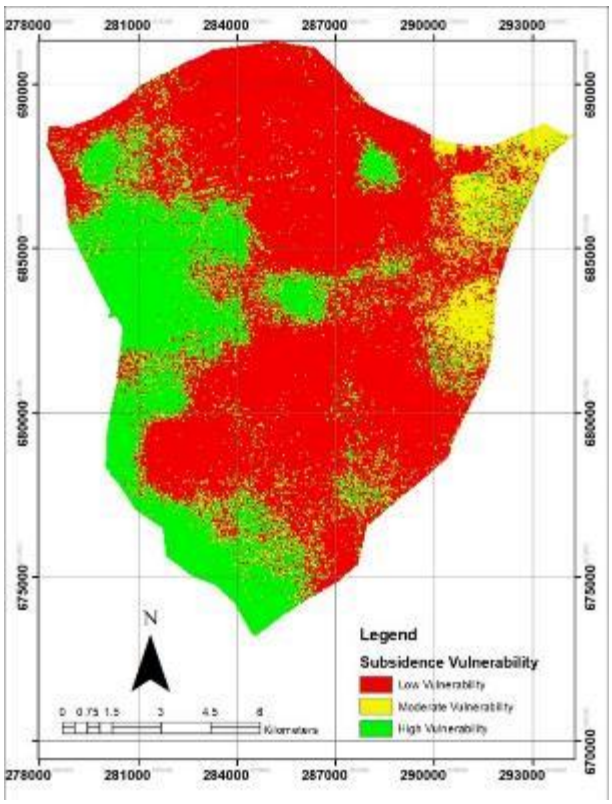

Figure 6 Awka South Land Subsidence Vulnerability

4. Discussion of Results

In this study, four Sentinel-1A SAR images were utilized to map the extent of land subsidence in Awka South. These images underwent a comprehensive series of InSAR processing steps to derive the TopoPhase and Coherence products. These products were subsequently terrain corrected using range Doppler terrain corrections, and the displacement was calculated from these corrected products.

The results indicated that the subsidence ranged from a minimum of 2.33 meters to a maximum of 9.76 meters in 2019, and from a minimum of 3.99 meters to a maximum of 11.22 meters in 2020, as illustrated in Figures 1, 2, and 3. The significant increase in subsidence from 2019 to 2020 highlights the dynamic nature of ground movements in Awka South.

The analysis showed a trend percentage of 6.95% and an annual rate of change of 3.47 meters per year, indicating an increasing trend in subsidence in Awka South. This finding suggests that land subsidence is a growing issue in the area, which could have significant implications for infrastructure, agriculture, and overall land stability. The net displacement movement data was reclassified into three vulnerability levels using natural breaks (Jenks method): high risk, moderate risk, and low risk. The percentages and areas covered by each risk level were extracted and analyzed. The results revealed that: - High-risk zones occupy 33% of the total area, spanning 5634.78 hectares. - Moderate-risk zones occupy 16.18%, covering 2763.47 hectares. - Low-risk zones occupy 50.82%, covering 8678.22 hectares. These findings are illustrated in Figures 5 and 6.

The increasing subsidence trend and the significant areas classified as high and moderate risk highlight the urgent need for mitigation measures in Awka South. The high-risk zones, in particular, are likely to face severe impacts on infrastructure and agricultural productivity if subsidence continues at the current rate. The moderate-risk zones, while less immediately threatened, also require attention to prevent escalation to high-risk status. The data and analysis presented in this study provide a crucial foundation for policymakers, urban planners, and environmental managers to develop targeted strategies to address land subsidence. Implementing measures such as improved water management, land-use planning, and structural reinforcements can help mitigate the effects of subsidence and protect vulnerable areas.

5. Conclusion

The comprehensive analysis of Sentinel-1A SAR data for Awka South has highlighted a significant and increasing trend of land subsidence between 2019 and 2020. With subsidence values ranging from 2.33 meters to 9.76 meters in 2019 and 3.99 meters to 11.22 meters in 2020, it is clear that the region is experiencing notable ground movements that pose serious risks to infrastructure, agriculture, and overall land stability.

The application of InSAR processing techniques, including TopoPhase, Coherence product derivation, and range Doppler terrain corrections, has enabled the accurate calculation of displacement and provided valuable insights into the extent and progression of subsidence in the area. The observed trend percentage of 6.95% and an annual rate of change of 3.47 meters per year underscore the urgency of addressing this issue.

The reclassification of land subsidence vulnerability into high, moderate, and low-risk zones using the natural breaks method (Jenks) has further revealed that 33% of the area is at high risk, 16.18% at moderate risk, and 50.82% at low risk. These findings are critical for guiding mitigation efforts and resource allocation.

Given the substantial areas identified as high and moderate risk, it is imperative for policymakers, urban planners, and environmental managers to develop and implement targeted strategies to mitigate the impacts of land subsidence. Measures such as improved water management, land-use planning, and structural reinforcements are essential to prevent further subsidence and protect vulnerable areas.

Compliance with ethical standards

Disclosure of conflict of interest

No conflict of interest to be disclosed.

References

[1] Galloway, D., & Burbey, T. J. (2011). Review: Regional land subsidence accompanying groundwater extraction. Hydrogeology Journal, 19(8), 1459-1486.

[2] Chaussard, E., Amelung, F., Abidin, H. Z., & Hong, S. H. (2013). Sinking cities in Indonesia: ALOS PALSAR detects rapid subsidence due to groundwater and gas extraction. Remote Sensing of Environment, 128, 150-161.

[3] Alozie, J. O., Otti, V. I., & Okoro, E. U. (2020). Environmental impact of land subsidence due to groundwater withdrawal in urban areas: Case study of Awka, Nigeria. Environmental Monitoring and Assessment, 192(6), 1-15.

[4] Ferretti, A., Prati, C., & Rocca, F. (2001). Permanent scatterers in SAR interferometry. IEEE Transactions on Geoscience and Remote Sensing, 39(1), 8-20.

[5] Raucoules, D., Le Mouelic, S., Carnec, C., King, C., & Hosford, S. (2009). Monitoring of slow ground deformation by ERS radar interferometry on the Vauvert salt mine (France)—comparison with ground-based measurement. Remote Sensing of Environment, 68(3), 409-422.

[6] Hanssen, R. F. (2001). Radar interferometry: Data interpretation and error analysis. Springer Science & Business Media.

[7] Hooper, A., Bekaert, D., Spaans, K., & Arıkan, M. (2012). Recent advances in SAR interferometry time series analysis for measuring crustal deformation. Tectonophysics, 514-517, 1-13.

[8] Tomás, R., Romero, R., Mulas, J., Marturià, J. J., Mallorquí, J. J., Lopez-Sanchez, J. M., ... & Herrera, G. (2014). Radar interferometry techniques for the study of ground subsidence phenomena: A review of practical issues through cases in Spain. Environmental Earth Sciences, 71, 163-181.

[9] Raspini, F., Ciampalini, A., Del Conte, S., Lombardi, L., Nocentini, M., Gigli, G., ... & Casagli, N. (2018). Exploitation of Landsat 8 and Sentinel-1 data for the detection of ground deformations and soil moisture variations in flood prone areas. Natural Hazards and Earth System Sciences, 18(5), 1485-1500.

[10] Olorunfemi, M. O., Ojo, J. S., Akintorinwa, O. J., & Idem, S. O. (2011). Hydrogeophysical evaluation of the groundwater potential of Akure metropolis, southwestern Nigeria. Journal of Mining and Geology, 47(2), 139-157.

[11] Galloway, D., Jones, D. R., & Ingebritsen, S. E. (1999). Land subsidence in the United States. US Geological Survey Circular 1182.

[12] Zhu, L., Ding, X., & Zhang, L. (2013). Correlation analysis of soil moisture changes from InSAR and GRACE: A case study in California, USA. International Journal of Remote Sensing, 34(18), 6454-6476.

[13] Ojha, C. S. P., & Kaur, R. (2014). Groundwater modelling and management. Springer.

[14] Massonnet, D., & Feigl, K. L. (1998). Radar interferometry and its application to changes in the Earth's surface. Reviews of Geophysics, 36(4), 441-500.

[15] Bawden, G. W., Thatcher, W., Stein, R. S., Hudnut, K. W., & Peltzer, G. (2001). Tectonic contraction across Los Angeles after removal of groundwater pumping effects. Nature, 412(6849), 812-815.

[16] Bell, J. W., Amelung, F., Ramelli, A. R., & Blewitt, G. (2002). Land subsidence in Las Vegas, Nevada, monitored by interferometric synthetic aperture radar imagery. Geophysical Research Letters, 29(13), 10-1.

[17] Fattahi, H., & Amelung, F. (2013). InSAR observations of ground subsidence in Salt Lake City, Utah: Evidence for aquifer-system compaction. Water Resources Research, 49(9), 6542-6556.

[18] Chen, J., Zebker, H. A., & Knight, R. (2015). Groundwater extraction monitoring with InSAR: Data accuracy and its impact on water management policy. Journal of Hydrology, 524, 612-623.

[19] Berardino, P., Fornaro, G., Lanari, R., & Sansosti, E. (2002). A new algorithm for surface deformation monitoring based on small baseline differential SAR interferograms. IEEE Transactions on Geoscience and Remote Sensing, 40(11), 2375-2383.

[20] Gabriel, A. K., Goldstein, R. M., & Zebker, H. A. (1989). Mapping small elevation changes over large areas: Differential radar interferometry. Journal of Geophysical Research: Solid Earth, 94(B7), 9183-9191.